PROCEEDINGS OF SPIE

SPIEDigitalLibrary.org/conference-proceedings-of-spie

Characterizing the cross dispersion reflection gratings of CRIRES+

Follert, Roman, Taubert, Dieter, Hollandt, Jörg, Monte, Christian, Oliva, Ernesto, et al.

Roman Follert, Dieter Taubert, Jörg Hollandt, Christian Monte, Ernesto Oliva, Ulf Seemann, Tom Löwinger, Heiko Anwand-Heerwart, Christof Schmidt, Reinhold J. Dorn, Paul Bristow, Artie Hatzes, Ansgar Reiners, Nikolai Piskunov, Ulrike Heiter, Eric Stempels, Thomas Marquart, Alexis Lavail, Claudio Cumani, Jason Grunhut, Andreas Haimerl, Renate Hinterschuster, Derek J. Ives, Yves Jung, Florian Kerber, Barbara Klein, Jean Louis Lizon, Ignacio Molina-Conde, Belinda Nicholson, Livia Origlia, Luca Pasquini, Jérôme Paufique, Jörg Stegmeier, Sebastien Tordo, "Characterizing the cross dispersion reflection gratings of CRIRES+," Proc. SPIE 9912, Advances in Optical and Mechanical Technologies for Telescopes and Instrumentation II, 99122B (1 August 2016); doi: 10.1117/12.2232569

SPIE.

Event: SPIE Astronomical Telescopes + Instrumentation, 2016, Edinburgh, United Kingdom

Characterizing the cross dispersion reflection gratings of CRIRES+

Roman Follert[a,*], Dieter Taubert[b], Jörg Hollandt[b], Christian Monte[b], Ernesto Oliva[c], Ulf Seemann[d], Tom Löwinger[a], Heiko Anwand-Heerwart[d], Christof Schmidt[h], Reinhold J Dorn[e], Paul Bristow[e], Artie Hatzes[a], Ansgar Reiners[d], Nikolai Piskunov[f], Ulrike Heiter[f], Eric Stempels[f], Thomas Marquart[f], Alexis Lavail[e,f], Claudio Cumani[e], Jason Grunhut[e], Andreas Haimerl[e], Renate Hinterschuster[e], Derek J Ives[e], Yves Jung[e], Florian Kerber[e], Barbara Klein[e], Jean Louis Lizon[e], Ignacio Molina-Conde[e], Belinda Nicholson[e], Livia Origlia[g], Luca Pasquini[e], Jérôme Paufique[e], Jörg Stegmeier[e], and Sebastien Tordo[e]

[a]Thüringer Landessternwarte Tautenburg, Sternwarte 5, 07778 Tautenburg, Germany
[b]Physikalisch-Technische Bundesanstalt, Fachbereich 7.3 Detektorradiometrie und Strahlungsthermometrie, Abbestraße 2-12, 10587 Berlin, Germany
[c]INAF Osservatori di Arcetri, Largo E. Fermi 5, 50125 Firenze, Italy
[d]Institut für Astrophysik, Georg-August-Universität Göttingen, Friedrich-Hund-Platz 1, 37077 Göttingen, Germany
[e]European Organisation for Astronomical Research in the Southern Hemisphere, Karl-Schwarzschild-Straße 2, 85748 Garching bei München, Germany
[f]Department for Physics and Astronomy, University of Uppsala, Box 515, 751 20 Uppsala, Sweden
[g]INAF Osservatorio di Bologna, Via Ranzani 1, 40127 Bologna, Italy
[h]Zentralwerkstatt Fakultät für Physik, Georg-August-Universität Göttingen, Friedrich-Hund-Platz 1, 37077 Göttingen, Germany

ABSTRACT

The CRIRES$^+$ project attempts to upgrade the CRIRES instrument into a cross dispersed echelle spectrograph with a simultaneous recording of 8-10 diffraction orders. In order to transform the CRIRES spectrograph into a cross-dispersing instrument, a set of six reflection gratings, each one optimized for one of the wavelength bands CRIRES$^+$ will operate in (YJHKLM), will be used as cross dispersion elements in CRIRES$^+$. Due to the upgrade nature of the project, the choice of gratings depends on the fixed geometry of the instrument. Thus, custom made gratings would be required to achieve the ambitious design goals. Custom made gratings have the disadvantage, though, that they come at an extraordinary price and with lead times of more than 12 months. To mitigate this, a set of off-the-shelf gratings was obtained which had grating parameters very close to the ones being identified as optimal. To ensure that the rigorous specifications for CRIRES$^+$ will be fulfilled, the CRIRES$^+$ team started a collaboration with the Physikalisch-Technische Bundesanstalt Berlin (PTB) to characterize gratings under conditions similar to the operating conditions in CRIRES$^+$ (angle of incidence, wavelength range).

The respective test setup was designed in collaboration between PTB and the CRIRES$^+$ consortium. The PTB provided optical radiation sources and calibrated detectors for each wavelength range. With this setup, it is possible to measure the absolute efficiency of the gratings both wavelength dependent and polarization state dependent in a wavelength range from 0.9 μm to 6 μm.

Keywords: CRIRES$^+$, echelle spectrograph, infrared instrumentation, VLT, diffraction efficiency

Further author information:
Roman Follert: E-mail: follert@tls-tautenburg.de, Telephone: +49 36427 863 48

Advances in Optical and Mechanical Technologies for Telescopes and Instrumentation II, edited by Ramón Navarro, James H. Burge, Proc. of SPIE Vol. 9912, 99122B
 · doi: 10.1117/12.2232569

1. INTRODUCTION

High-resolution infrared (IR) spectroscopy plays an important role in astrophysics from the search for exoplanets to cosmology. The majority of currently existing IR spectrographs are limited by their small simultaneous wavelength coverage. The scientific community has recognized the need for large wavelength range, high-resolution IR spectrographs, and several are currently either in the design, integration phase or at the telescope. Examples are ISHELL[1] at the NASA Infrared Telescope Facility, SPIROU[2] for the Canada France Hawaii Telescope (CFHT) and CARMENES for the Calar Alto Observatory.[3]

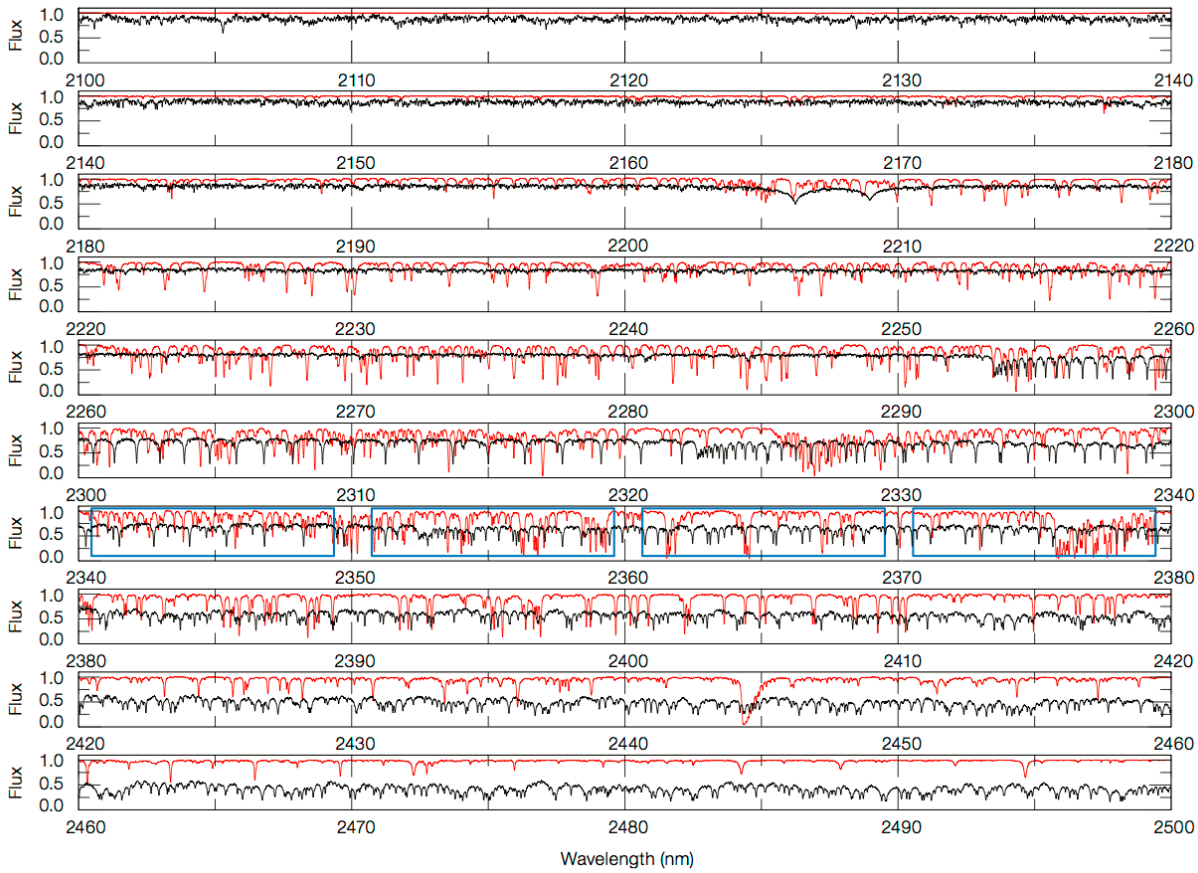

Figure 1: The wavelength coverage of the old CRIRES (blue boxes correspond to the four Aladdin detectors) in the K-band compared to the expected coverage of a single exposure from CRIRES$^+$. The black line shows the spectrum of an M4 dwarf star (0.15 $M_\odot$) and the red line is a laboratory spectrum of a gas cell prototype[4,5] for CRIRES$^+$ being developed at the University of Göttingen.

The adaptive optics (AO) assisted CRIRES instrument, previously installed at the European Southern Observatory Very Large Telescope (ESO VLT, Cerro Paranal, Chile), was an IR (0.92 μ - 5.2 μm) high-resolution spectrograph which was in operation from 2006 to 2014. CRIRES was a unique instrument, accessing a parameter space (wavelength range and spectral resolution), which up to now was largely uncharted, as described in Käufl et al. (2004)[6] and for the AO system by Paufique et al. (2004).[7] In its setup, it consisted of a single order spectrograph providing long-slit (40 arcsecond) spectroscopy with a resolving power up to R=100 000.

However, the setup was limited to a narrow, single-shot, spectral range of about 1/70 of the central wavelength, resulting in low observing efficiency for many modern scientific programs requiring a broad spectral coverage. By introducing cross dispersing elements and larger detectors, the simultaneous wavelength range can be increased by a factor of ten with respect to the old configuration, while the total operational wavelength range can be preserved (see Figure 1).

The CRIRES$^+$ project[8,9,10] attempts to upgrade the CRIRES instrument, this will turn CRIRES$^+$ into a fully operational cross dispersed echelle spectrograph[11,12] with a simultaneous recording of 8-10 diffraction orders. One of the main design goals of the upgrade project is to at least maintain or to increase the overall throughput of the instrument. To achieve this ambitious goal, all components will be optimized for their task and rigorously tested before integration.

In order to transform the CRIRES spectrograph into a cross-dispersing instrument, a set of six reflection gratings, each one optimized for one of the wavelength bands CRIRES$^+$ will operate in (YJHKLM), will be used as cross dispersion elements in CRIRES$^+$. Due to the upgrade nature of the project, the choice of gratings depends on the fixed geometry of the instrument. Thus, custom made gratings would be required to achieve the ambitious design goals. Custom made gratings have the disadvantage, though, that they come at an extraordinary price and with lead times of more than 12 month. To mitigate this, a set of off-the-shelf gratings was obtained which had grating parameters very close to the ones being identified as optimal. To ensure that the rigorous specifications for CRIRES$^+$ will be fulfilled, the CRIRES$^+$ team started a collaboration with the the Physikalisch-Technische Bundesanstalt Berlin (PTB) to characterize gratings under conditions similar to the operating conditions in CRIRES$^+$ (angle of incidence, wavelength range).

The respective test setup was designed in collaboration between the PTB and the CRIRES$^+$ consortium. It consist mainly of bulk optics and is operated at room temperatures. The PTB, the national metrology institute of Germany, provided optical radiation sources and calibrated detectors for each wavelength range. With this setup, it is possible to measure the absolute efficiency of the gratings both wavelength dependent (nine different wavelength equally distributed in each band) and polarization state dependent (the setup is equipped with a polarimetry unit) in a wavelength range from 0.9 μm to 6 μm.

We will present in this paper a description of test setup, including a discussion of the lessons learned, and the test results on a set of off-the-shelf gratings.

2. DESCRIPTION OF THE LAB SETUP

In this section, we will first describe the gratings which were characterized in the work presented here (see subsection 2.1), then, we will give a detailed description of the test setup (see subsection 2.2).

2.1 Characterized gratings

In order to identify gratings suitable for the demanding requirements of the CRIRES$^+$ technical specifications, a set of six gratings was bought from a major grating manufacturer and characterized. Table 1 gives the main parameters of these gratings. The substrates of the gratings consist of thermally treated Al6061 and have a dimension of 68.6 mm $\times$ 68.6 mm $\times$ 9.1 mm. The ruled area of each grating has a size of 64 mm $\times$ 64 mm and is gold coated.

For the Y band (0.95 – 1.1 μm), no suitable grating could be identified. For the K band, two possibly suitable gratings were identified, K_1 and K_2, both were ordered and characterized.

Table 1: Main parameters of the CRIRES$^+$ cross-dispersion gratings. α is the angle of incidence perpendicular to the dispersion direction (non Littrow configuration).

Wavelength band	Wavelength range [μm]	ll / mm	Angle of incidence α [°]	Blaze Angle [°]
J	1.13 – 1.36	400	14.6	15.0
H	1.48 – 1.81	235.8	11.3	9.25
K_1	1.93 – 2.54	150	9.7	8.6
K_2	1.93 – 2.54	150	9.7	10.8
L	2.85 – 4.20	58	6.1	6.0
M	3.58 – 5.62	40	5.4	5.5

The manufacturer provided a characterization of all of the gratings specified in Table 1, for some even polarization resolved. Unfortunately, for most of them the measurements of the manufacturer were performed at higher dispersion orders and in a different optical setup then anticipated for CRIRES$^+$. Therefore, the data provides only some potential to forecast the efficiency of the gratings at CRIRES$^+$ operating conditions.

2.2 Description of the current test setup

The absolute spectral diffraction efficiency of each grating results from a spectrally resolved ratio measurement between the grating under test and the known spectral reflectance of a reference mirror.

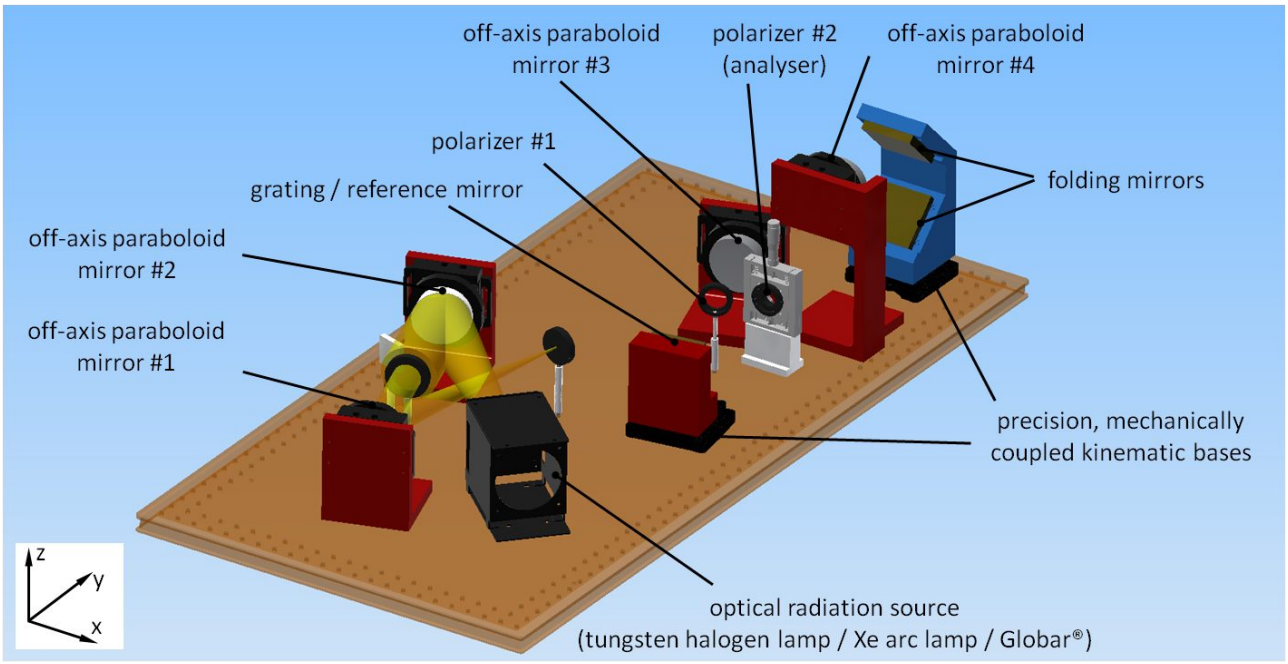

Figure 2: 3D Model of the AGEM. The light from the radiation source is first collimated by the off-axis paraboloid #1, which is followed by a variable diameter circular aperture determining the collimated beam diameter of the setup. The beam is then re-focused by the off-axis paraboloid #2 on a pinhole for modal filtering (lower left of the Figure). Then, the beam is re-collimated again by the off-axis paraboloid #3. The beam passes next through the first polarizer (#1) before being reflected from either the grating or the reference mirror mounted on a high precision, mechanically coupled kinematic mount for easy and reproducible exchange. Next the beam goes through the second polarizer(#2) to ensure the correct polarization state. The latter, serving as an analyzer is mounted on a vertical translation stage in order to correct for the dispersion borne beam displacement. The wavelength to be measured at is selected via one of nine custom made folding mirror mounts carrying two flat mirrors (see also Figure 3). Finally, the last off-axis paraboloid #4 focuses the beam such that it fits the focal point of the SRCF (not depicted).

The applied setup consisted of the PTB Apparatus for Grating Efficiency Measurement (AGEM) depicted in Figure 2 in conjunction with the PTB Spectral Radiance Comparator Facility (SRCF). The SRCF served as the spectrally resolving detector unit by applying a double grating monochromator with a variety of photodiodes as detectors (see Table 2). The basic components of the AGEM are the radiation source, the opto-mechanical components for beam forming (off-axis paraboloid mirrors) and a breadboard mounting for the precise alignment of components. We used either a Tungsten halogen lamp (for NIR wavelength), a Xe arc lamp radiation source in conjunction with a sapphire window or a Globar®-type radiation source for the longer (> 3 μm) wavelength range. The gratings and the reference mirror were mounted on individual, high precision machined holders; the orientation of the grating grooves was parallel to the surface of the optical breadboard (x-y plane), hence, the dispersion plane of the gratings was set in the y-z plane (see Figure 2).

To achieve a good positioning reproduceability when interchanging between any grating and the reference mirror for the ratio measurement, high precision, mechanically coupled kinematic bases were used for mounting. The AGEM was aligned such that with the reference mirror in the setup the exit focal point and optical axis would match the entrance focal point and optical axis of the SRCF.

Table 2: Types of photo detectors used in the SRCF.

Type of photo diode	wavelength range [μm]
InGaAs	1 – 1.7
InSb	1.4 – 5
HgCdTe	5 – 7

In the most recent version of the AGEM, two thin film linear polarizers ($\lambda<2$ μm) respective two wire grid linear polarizers based on a KRS-5 substrate ($\lambda>2$ μm) have been included in order to be able to measure the polarized wavelength dependent efficiency of the grating perpendicular and parallel to the grating grooves. The polarizers have an accessible aperture of 1 inch (25.5 mm), which slightly obstructs the parallel beam (38 mm). This was accepted due to the direct availability of the polarizers from a former experiment. In addition, it is not expected that the grating efficiency varies significantly on scales larger than this.

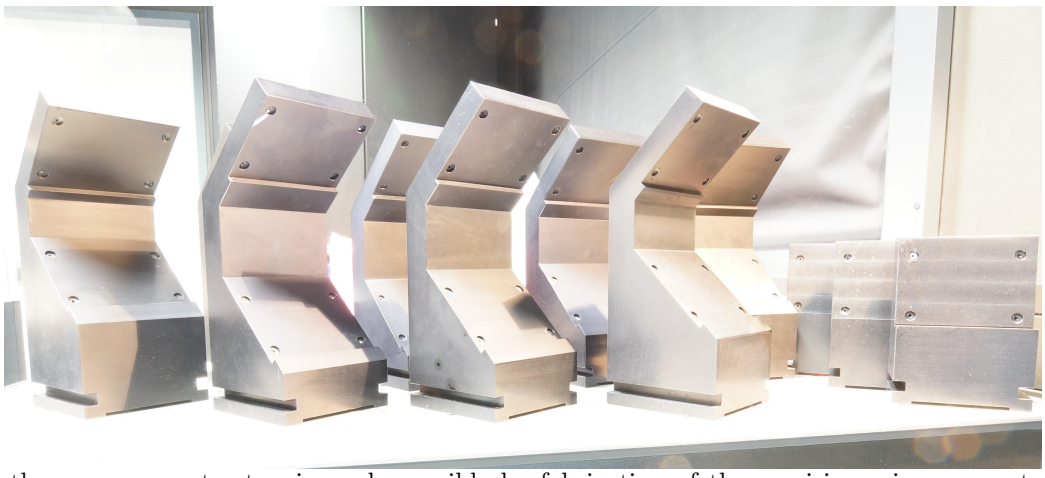

Figure 3: the measurement setup is made possible by fabrication of the precision mirror mounts employing wire-electro discharge machining. This technique easily excels the required tolerances of better than $\pm$ 0.05 mm and angularly better than $\pm$ 0.03°.

The wavelength selection for the measurements including the grating was achieved by means of nine different folding mirror pair holders (see Figure 3). For each of these V-shaped mounts, the distance and respective angle between the two mounted mirrors was carefully precision machined. By choosing a defined angular position (y-axis as the rotation axis) and the vertical position (z-axis as the translational axis) for each of the two folding mirrors, the matching conditions of the focal points and the optical axis of AGEM and SRCF are valid for one wavelength only. The design of the folding mirror holders was set to obtain nine approximately equidistant

wavelength measurement points over the entire band of operation of the respective grating. Prior to the absolute grating efficiency measurements, the corresponding wavelengths for every grating / folding mirror combination were accurately determined by performing a SRCF wavelength scan.

To correct for a possible drift of the optical power of the radiation source between the measurements of the grating or the reference mirror, a temperature controlled (30°C) extended InGaAs photodiode was inserted as a monitor detector into the unused sector of the collimated beam path by means of a beam splitter.

The absolute spectral diffraction efficiency of each grating $\eta(\lambda)$ was calculated according to Equation 1.

$$\eta(\lambda) = R_{ref}(\lambda) \times \frac{I_{grating}(\lambda) - I_{dark}(\lambda)}{I_{ref}(\lambda) - I_{dark}(\lambda)} \times \frac{I_{monitor,ref}(\lambda)}{I_{monitor,grating}(\lambda)} \times \frac{R_{fold,ref}(\lambda)}{R_{fold,grating}(\lambda)} \quad (1)$$

with:

$R_{ref}(\lambda)$	spectral reflectance of the reference mirror
$I_{grating}(\lambda)$	detector signal – grating measurement
$I_{ref}(\lambda)$	detector signal – reference mirror measurement
$I_{dark}(\lambda)$	detector signal – dark measurement
$I_{monitor,grating}(\lambda)$	monitor detector signal – grating measurement
$I_{monitor,ref}(\lambda)$	monitor detector signal – reference mirror measurement
$R_{fold,grating}(\lambda)$	spectral reflectance folding mirror pair – grating measurement
$R_{fold,ref}(\lambda)$	spectral reflectance folding mirror pair – reference mirror measurement

2.3 Description of measurement procedure

We applied the following measurement procedure to obtain the wavelength dependent diffraction efficiency of each grating in order to minimize systematic effects:

1. Set both polarizers to parallel to the grating grooves (x-y plane respectively)
2. Put grating on grating mount and first folding mirror (associated with λ_1) mount in setup.
3. Measure both $I_{monitor,grating}(\lambda_1)$ and $I_{grating}(\lambda_1)$
4. Insert an optical shutter in the beam and measure detector dark signal $I_{dark}(\lambda_1)$
5. Exchange grating mount with reference mirror mount and remove optical shutter
6. Measure both $I_{monitor,ref}(\lambda_1)$ and $I_{ref}(\lambda_1)$
7. Exchange reference mirror mount for grating mount and folding mirror mount for next folding mirror mount (associated with (associated with λ_2)
8. Start at step 3. again and repeat for all nine folding mirror mounts
9. Change both polarizers to perpendicular to the grating grooves (x-y plane respectively)
10. Repeat steps 2. to 8.

This procedure was repeated a few times at selected wavelengths (for selected folding mirror mounts respectively) to identify systematic effects.

3. RESULTS OF THE GRATING CHARACTERIZATION

In this section we will first present the results gathered in the two measurement campaigns (first half of 2015 and first half of 2016). We will also present a rigorous discussion of the systematic uncertainties which have been considered in the uncertainty bduget.

3.1 Results of the characterization campaign

Figure 5 below shows the results of the CRIRES$^+$ grating characterization campaign. We present the dispersion efficiencies of six gratings. For a detailed description of the measurement procedure see section 2.3. For a detailed discussion of the uncertainties see section 3.2. For each grating we present the wavelength dependent absolute dispersion efficiency parallel to the grating grooves (P mode, in blue), the wavelength dependent absloute dispersion efficiency perpendicular to the grating grooves (S mode, in green) and the mean wavelength dependent absolute dispersion efficiency (in red). In addition, we present data taken without the two linear polarizers in the beam (in black).

In addition to the set of the six gratings ordered in 2014, we ordered an additional set of three gratings (K2, L and M) of the same manufacturer, with the same specifications, as spares. At the time this work was published, only data for one of these gratings was available (K2). In Figure 4 we show the difference between the two K2 gratings for both the P mode, S mode and the mean absolute dispersion efficiency.

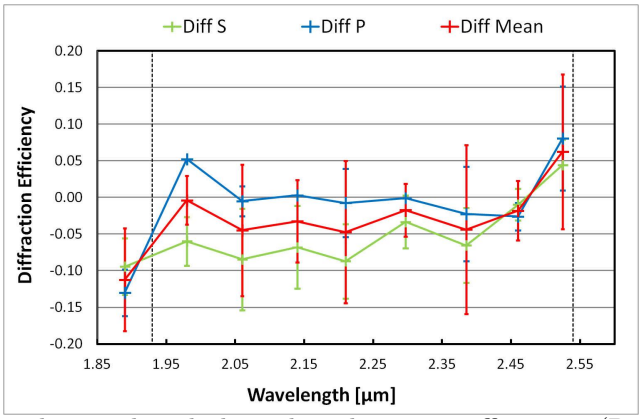

Figure 4: Difference between the wavelength dependent dispersion efficiencies (P mode, S mode and mean) of the K2 gratings from the 2016 and the 2014 order.

3.2 Discussion of uncertainty contributions

The relative uncertainty contributions and the corresponding combined relative standard uncertainty ($k = 1$) of the measured absolute efficiencies for the gratings J, H, K1, K2, L and M are given in Table 3. The main uncertainty components are contributions arising from the reproducibility ($u_{repr,rel}$), the reference mirror absolute reflectance ($u_{RefMir,rel}$), the radiation source drift($u_{drift,rel}$) and the detector / amplifier noise ($u_{noise,rel}$), they are listed below in the approximate order of their magnitude.

The reproducibility uncertainty contribution $u_{repr,rel}$ was estimated by repeated measurements at selected wavelengths which included the manual removal and repositioning of the grating under investigation respectively as well as the reference mirror and the folding mirror unit from / to their kinematic bases. As the measurement method requires also the rotation of the polarizers, due to their imperfect optical surfaces of the latter, a slight, random angular displacement of the optical beam in the diffraction plane cannot be completely avoided leading to a random wavelength shift hence to random variation of the determined grating efficiency. This effect is included in the reproducibility uncertainty component and was estimated by a repeated measurements including the back and forth 90° rotation of the polarizers around their optical axis.

The absolute dispersion efficiency is based on the absolutely calibrated reflectance of the reference mirror, the calibration being performed on a dedicated PTB facility. For the wavelength range from 1 μm to 6 μm, the relative standard uncertainty of the reference mirror reflectance $u_{RefMir,rel}$ is estimated to be on average 2%. This uncertainty includes also the reflectance variation between the plane mirrors used in the folding mirror

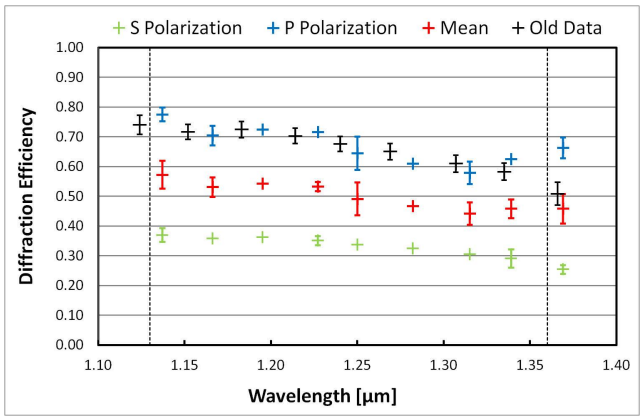

(a) Diffraction Efficiency J Band grating.

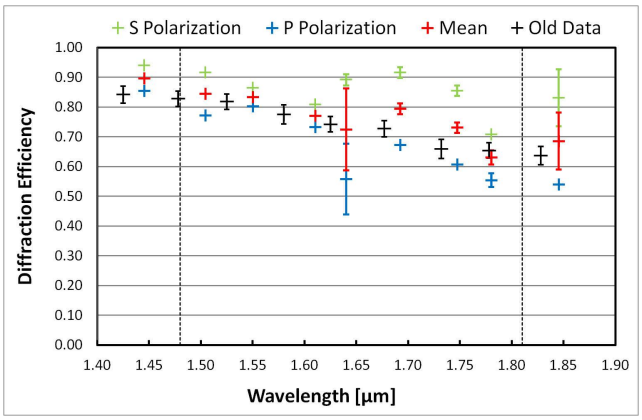

(b) Diffraction efficiency H band grating.

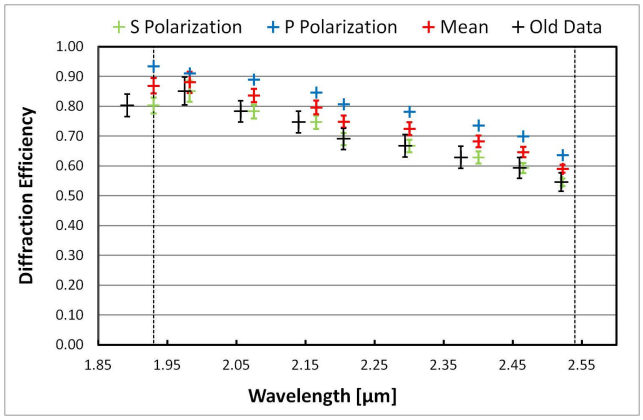

(c) Diffraction efficiency K band grating (K1).

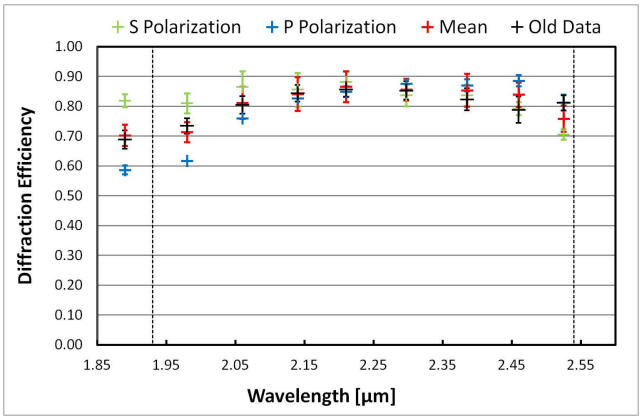

(d) Diffraction efficiency K band grating (K2).

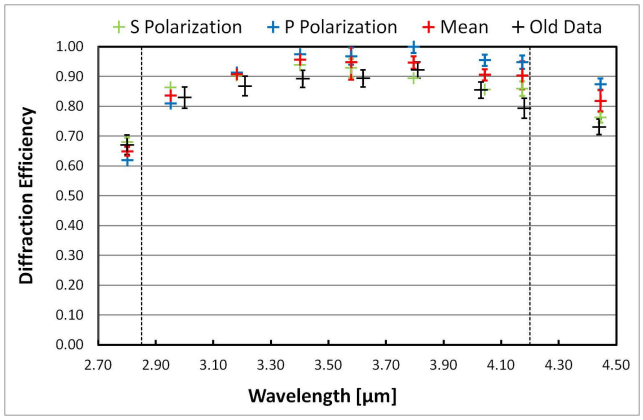

(e) Diffraction efficiency L band grating.

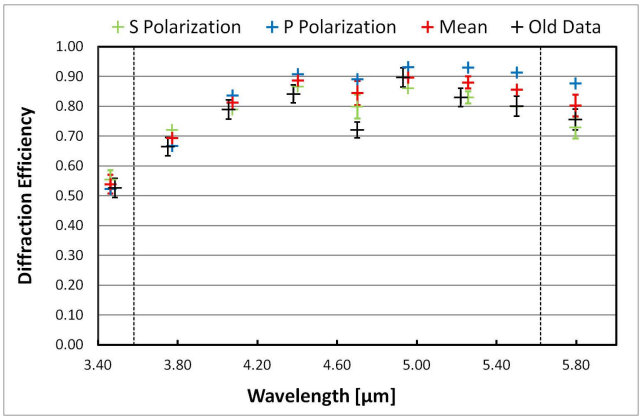

(f) Diffraction efficiency M band grating.

Figure 5: Results of the CRIRES$^+$ gratings characterization campaign. For a detailed description of the gratings see Table 1. In each subfigure, blue crosses denote the absolute dispersion efficiency in a linear polarization state parallel to the grating grooves (P mode), green crosses denote the absolute dispersion efficiency in a linear polarization state perpendicular to the grating grooves (S mode), the red crosses denote the mean absolute dispersion efficiency and the black crosses denote the data taken in the first characterization campaign. Uncertainty bars are only given for data points where the error due to reproducibility has been determined. See also subsection 3.2 for a discussion of the errors.

Table 3: Components of the uncertainty associated with the measurments. We present the average uncertainty of each component and the respective statistic distribution of the components. The last row than gives the combined average uncertainty for each wavelength band / grating.

Uncertainty component			Wavelength band					
		Distribution	J	H	K1	K2	L	M
reproducibility	$u_{repr,rel}$	normal	2.9	7.8	5.4	2.1	1.5	3.9
reflectance reference mirror	$u_{RefMir,rel}$	normal	2.0	2.0	2.0	2.0	2.0	2.0
radiation source drift	$u_{drift,rel}$	rectangular	0.03	0.02	0.02	0.02	0.35	0.54
noise	$u_{noise,rel}$	normal	0.02	0.02	0.01	0.02	0.16	0.53
combined standard uncertainty (k=1)			3.5	8.0	5.8	2.9	2.5	4.5

units. These variations are estimated to be negligible, as all plane mirrors, including the reference mirror are from the same manufacturing batch.

The drift of the optical radiation source of AGEM between the step 3 and step 6 of the measurement procedure (see Section 2.3) is corrected via the respective simultaneously measured photocurrents $I_{monitor,ref}(\lambda)$ and $I_{monitor,grating}(\lambda)$ of the monitor photodiode according to Equ. 1. As the monitor photo diode is a broadband detector (extended InGaAs), the correction factor applied is a spectrally integrated value over the spectral responsivity of the monitor detector. Therefore, to consider the possible deviation between the spectral drift and integrated drift of the radiation source, the correction factor itself is considered as an additional uncertainty component $u_{drift,rel}$ (rectangular distribution).

The measurement procedure comprised the measurement of the respective photocurrents of detectors applied at the SRCF. Typically 30 single measurements were taken for $I_{grating}$, I_{ref} and I_{dark} (Equ. 1). The relative uncertainty $u_{noise,rel}$, accounting for the noise of the selected detector/ amplifier combination, was calculated on the basis of the standard deviation of the mean of the single measurements.

4. DISCUSSION OF RESULTS

The results presented in Section 3 served three purposes:

1. To identify suitable gratings for CRIRES$^+$
2. To properly model the instrument
3. To serve as input for the data reduction pipeline of CRIRES$^+$

Since CRIRES$^+$ is an upgrade to an existing instrument, we were severely limited in the optical design[11] by the mechanical structures of CRIRES. Therefore, the first optical design suggested to use only custom made newly ruled gratings. Since such gratings are significantly more expensive than common replica gratings ($\approx$ a factor of 20-30), the instrument team was investigating means to test the suitability of gratings for CRIRES$^+$ early on in the project. The results gathered in the first characterization campaign in early 2015 (black crosses in Figure 5) were already sufficient to achieve this goal. The CRIRES$^+$ instrument team specified that a) all gratings should have an average (averaged over the band of operation) efficiency of larger than 65% and b) the efficiency in the band of operation should drop nowhere below 55%. Due to the first characterization campaign, PTB and the CRIRES$^+$ instrument team were able to identify the K2, L and M gratings as suitable for CRIRES$^+$. This is also the reason why a set of spares for these gratings was ordered and is currently characterized. Note that the H band grating also nominally fulfills these criteria, but the instrument team decided to provide a custom made grating in addition. This custom made grating will have its blaze wavelength in the center of the H band and thus should have a larger average efficiency in the H band. The grating presented here will serve as a fallback solution, though.

To fulfill the the second and third goals of the characterization campaign, we will continue the work until the end of this year. In fall 2016 the custom made gratings for the Y, J and H bands should become available, they will then be also characterized accordingly. Thus, by the end of the year, we will have, for each of the CRIRES$^+$ cross dispersion gratings, the wavelength dependent absolute dispersion efficiency both in S and P mode. This will first of all allow us to model the system behavior of CRIRES$^+$ and thus give us the option to make reliable predictions on the efficiency of the entire instrument. The data will also allow us to disentangle systematic effects when calibrating the CRIRES$^+$ instrument and can serve as a time invariant quality control parameter. Furthermore, the data will also serve as input to the dedicated CRIRES$^+$ data reduction software suite, which is developed in parallel with the instrument. This will allow the user of the instrument in the end to reach the real limits of the instrument. Note that CRIRES$^+$ also provides a polarization mode[13] (both circularly and linearly polarized spectra will be available).

Last but not least, the PTB and the CRIRES$^+$ instrument team have developed a lab setup to easily and reproducably characterize reflection gratings both in S and P modes. Furthermore, the setup can easily be adapted to any optical configuration of any instrument, and can thus be widely applied to characterize gratings of other instruments. This allows for the first time to characterize the wavelength dependent absolute dispersion efficiency (S and P mode separate) of any grating of any manufacturer at any wavelength and in the respective optical configuration in a cheap and quick way. This is especially useful as most manufacturers rarely provide this information for their products.

ACKNOWLEDGMENTS

The German partners of the CRIRES$^+$ consortium are funded via grants (FKZ05A14ST1 and FKZ05A14MZ4) of the German Ministry of Education and Research (BMBF).

Valuable technical support C. Baltruschat and B. Prußeit is very much appreciated.

REFERENCES

[1] J. Rayner, T. Bond, M. Bonnet, *et al.*, "iSHELL: a 1-5 micron cross-dispersed R=70,000 immersion grating spectrograph for IRTF," in *Ground-based and Airborne Instrumentation for Astronomy IV*, *Proc. SPIE* **8446**, 84462C (2012).

[2] X. Delfosse, J.-F. Donati, D. Kouach, *et al.*, "World-leading science with SPIRou - The nIR spectropolarimeter / high-precision velocimeter for CFHT," in *SF2A-2013: Proceedings of the Annual meeting of the French Society of Astronomy and Astrophysics*, L. Cambresy, F. Martins, E. Nuss, *et al.*, Eds., 497–508 (2013).

[3] A. Quirrenbach, P. J. Amado, W. Seifert, *et al.*, "CARMENES. I: instrument and survey overview," in *Ground-based and Airborne Instrumentation for Astronomy IV*, *Proc. SPIE* **8446**, 84460R (2012).

[4] U. Seemann, G. Anglada-Escude, D. Baade, *et al.*, "Wavelength calibration from 1-5μm for the CRIRES+ high-resolution spectrograph at the VLT," in *Ground-based and Airborne Instrumentation for Astronomy V*, *Proc. SPIE* **9147**, 91475G (2014).

[5] U. Seemann, H. Anwand-Heerwart, P. Bristow, *et al.*, "The VLT/CRIRES+ calibration unit: design, integration, and test results including a novel Fabry-Perot etalon for wavelength calibration from 1-5μm," in *Ground-based Instrumentation for Astronomy*, *Proc. SPIE* **9908** (2016).

[6] H.-U. Kaeufl, P. Ballester, P. Biereichel, *et al.*, "CRIRES: a high-resolution infrared spectrograph for ESO's VLT," in *Ground-based Instrumentation for Astronomy*, A. F. M. Moorwood and M. Iye, Eds., *Proc. SPIE* **5492**, 1218–1227 (2004).

[7] J. Paufique, P. Biereichel, R. Donaldson, *et al.*, "MACAO-CRIRES: a step toward high-resolution spectroscopy," in *Advancements in Adaptive Optics*, D. Bonaccini Calia, B. L. Ellerbroek, and R. Ragazzoni, Eds., *Proc. SPIE* **5490**, 216–227 (2004).

[8] R. Follert, R. J. Dorn, E. Oliva, *et al.*, "CRIRES+: a cross-dispersed high-resolution infrared spectrograph for the ESO VLT," in *Ground-based and Airborne Instrumentation for Astronomy V*, *Proc. SPIE* **9147**, 914719 (2014).

[9] R. J. Dorn, G. Anglada-Escude, D. Baade, *et al.*, "CRIRES+: Exploring the Cold Universe at High Spectral Resolution," *The Messenger* **156**, 7–11 (2014).

[10] R. Dorn, P. Follert, R.and Bristow, C. Cumani, *et al.*, "The "+" for CRIRES: enabling better science at infrared wavelength and high spectral resolution at the ESO VLT," in *Ground-based Instrumentation for Astronomy*, *Proc. SPIE* **9908** (2016).

[11] E. Oliva, A. Tozzi, D. Ferruzzi, *et al.*, "Concept and optical design of the cross-disperser module for CRIRES+," in *Ground-based and Airborne Instrumentation for Astronomy V*, *Proc. SPIE* **9147**, 91477R (2014).

[12] J. L. Lizon, B. Klein, E. Oliva, *et al.*, "Opto-mechanical design of a new cross dispersion unit for the CRIRES+ high resolution spectrograph for the VLT," in *Ground-based and Airborne Instrumentation for Astronomy V*, *Proc. SPIE* **9147**, 91477S (2014).

[13] M. Lockhart, N. Piskunov, E. Stempels, *et al.*, "Novel infrared polarimeter for the ESO CRIRES+ instrument," in *Ground-based and Airborne Instrumentation for Astronomy V*, *Proc. SPIE* **9147**, 91478P (2014).